EurJIC European Journal of Inorganic Chemistry

ChemPubSoc Europe

FULL PAPER

DOI:10.1002/ejic.201300633

The Chelating Behaviour of 3-(4-X-Phenyl)-2-sulfanylpropenoic Acids with the Pb^{II} Ion – Relevance of the Lone Electron Pair in the Supramolecular Structures of the 2:1 Complexes

José S. Casas,[a] M. Victoria Castaño,*[a] Maria D. Couce,*[b] Agustín Sánchez,[a] José Sordo,[a] M. Dolores Torres,[a] and Ezequiel M. Vázquez López[b]

Dedicated to Professor Antonio Laguna on the occasion of his 65th birthday

Keywords: Lead / Chelates / Supramolecular chemistry / Lone electron pairs

The interaction of 3-(4-X-phenyl)-2-sulfanylpropenoic acids [H_2(X-pspa); X = –F, –Cl, –Br, –I, –OCH_3, –OCF_3, –OH] with lead(II) acetate in an alcoholic medium was explored in the search for new chelating agents for the Pb^{2+} ion. The direct reactions afforded [Pb(X-pspa)] complexes in yields of 67 (X = –Br) to 95 % (X = –OCH_3). When the Pb^{II}/H_2(X-pspa) reaction was performed in the presence of diisopropylamine (Q), the derivatives $[HQ]_2[Pb(X\text{-}pspa)_2]$ (X = Cl, Br) were obtained. All of the complexes were characterized by spectrometric (FAB-MS and ESI-MS) and spectroscopic (IR, ^1H and ^{13}C NMR spectroscopy) methods and these showed the permanence of the O,S coordination of the ligands to the metal ion in dimethyl sulfoxide (DMSO) solution. H_2(Cl-pspa), $[HQ]_2[Pb(Cl\text{-}pspa)_2]$ and $[HQ]_2[Pb(Br\text{-}pspa)_2]$ were also fully characterized in the solid state by X-ray diffraction. The importance of the stereochemically active lone electron pair of the Pb^{II} ion in the supramolecular arrangement of $[HQ]_2[Pb(X\text{-}pspa)_2]$ (X = Cl, Br) is discussed.

Introduction

"Inorganic lead" poisoning [i.e., intoxication with lead(II) derivatives] remains a serious occupational and environmental hazard.[1] The presence of this ion in mammals is known to provoke dysfunction in the renal, cardiovascular, reproductive and central nervous systems.[2] In children, a particularly sensitive section of the population, Pb^{II} ions may cause reduced growth and neuropsychological deficits even at very low metal blood levels.[3]

Chelation therapy is the usual clinical approach to reduce the body burden of lead in poisoned individuals.[4] Several examples of the drugs that are currently considered for the treatment of lead(II) decorporation are shown in Scheme 1.[5]

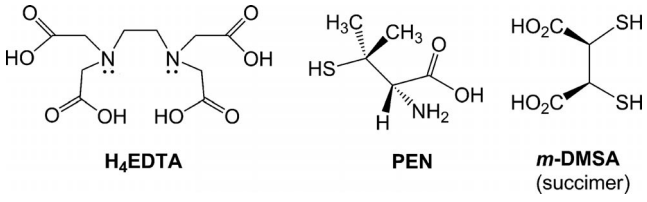

Scheme 1.

The compounds shown in Scheme 1 were not designed to mobilize specifically the lead(II) ion and none fulfil the characteristics required for an ideal chelating agent.[6] Thus, the preparation of new and more effective antidotes to treat Pb^{II} poisoning remains an important goal.

To achieve this goal, it is very important to consider the coordination preferences of the Pb^{II} cation. In this respect, the chelating agents shown in Scheme 1 constitute a rather heterogeneous group of ligands. For example, fully or partially deprotonated ethylenediaminetetraacetic acid (H_4EDTA) chelates the metal ion through the two aminic N atoms and four carboxylic O atoms, one from each carboxylate group.[7] In [Pb(PEN)] (PEN = D-penicillaminato), the ligand is N,O,S tridentate in the solid state.[8] In turn, the *meso*-2,3-dimercaptosuccinato ligand (*m*-$DMSA^{4-}$) binds Pb^{II} ions through one O atom and two S atoms in

[a] Departamento de Química Inorgánica, Universidade de Santiago de Compostela,
Campus Vida, 15782 Santiago de Compostela, Galicia, Spain
E-mail: mvictoria.castano@usc.es
[b] Departamento de Química Inorgánica, Universidade de Vigo, 36310 Vigo, Galicia, Spain
Fax: +34-986812556
E-mail: delfina@uvigo.es

Supporting information for this article is available on the WWW under http://dx.doi.org/10.1002/ejic.201300633.

© 2013 Wiley-VCH Verlag GmbH & Co. KGaA, Weinheim

aqueous solution.[9] Nevertheless, this variety of coordination modes is probably consistent with the behaviour of Pb^{II} ions as a borderline acid according to the hard and soft acids and bases (HSAB) principle of Pearson.[10]

However, although Pb^{II} ions are eclectic in terms of coordination mode, one would expect Pb^{II} ions to have a favoured combination of donor atoms. In this respect, it was pointed out that mixed O,S donor ligands may have the optimal hard/soft Lewis basicity to match the preferences of the lead(II) ion.[11] This is the chelating mode of DMSA and this may be the reason why this antidote has been recommended as a first choice chelator in cases of low-to-moderate lead(II) poisoning.[5]

In the search for new and better O,S donor molecules, we have explored the interaction of lead(II) with several 3-(4-X-phenyl)-2-sulfanylpropenoic acids [H_2(X-pspa), see Scheme 2], at present only from the point of view of coordination.

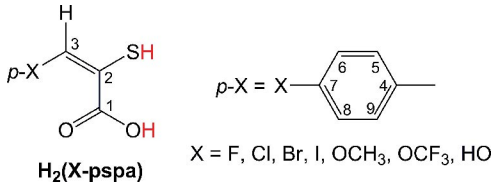

Scheme 2.

It would be expected that these compounds would bind to the Pb^{II} ion to form O,S chelates once their –COOH and –SH groups are deprotonated. It is also reasonable to expect that the *para*-X groups would have some influence on the electron charge on the donor atoms and the bioavailability of the compounds in biological media. The presence of the phenyl group will also possibly favour the liposolubility of the ligand and increase its ability to cross the cell membrane. H_2(I-pspa) behaves as a neuroprotective agent because it inhibits calpain, a class of protease located within the cell, in the cytosol.[12]

We describe here the solubility and spectroscopic and structural characteristics of the Pb^{II} complexes formed by H_2(X-pspa) To the best of our knowledge, previous research in this field has been limited to the preparation of the related Pb^{II} complexes with 3-(2-furyl)-2-sulfanylpropenoic acid,[13] 3-(phenyl)-2-sulfanylpropenoic acid[14] and 3-(phenyl)-3-(methyl)-2-sulfanylpropenoic acid.[15]

Results and Discussion

Synthesis and Properties of the Complexes

The reaction of $Pb(OAc)_2 \cdot 3H_2O$ and H_2(X-pspa) (1:1 molar ratio) in a mixture of EtOH/H_2O almost immediately afforded coloured solids with the [Pb(X-pspa)] stoichiometry (Scheme 3) in yields from 67 (X = –Br) to 95% (X = $–OCH_3$). All of the solids are insoluble in water and commonly used organic solvents except for dimethyl sulfoxide (DMSO) and dimethylformamide (DMF), in which they are sparingly soluble. All of the complexes melt with decomposition at temperatures close to 200 °C, except for the hydroxy derivative (X = –OH), which melted at 150 °C.

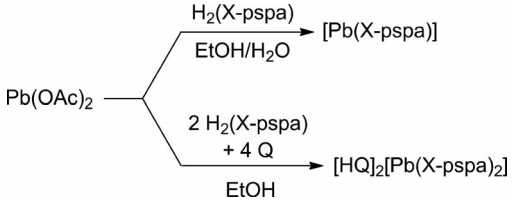

Scheme 3.

The reaction of lead(II) acetate with H_2(X-pspa) in the presence of diisopropylamine (Q) in a molar ratio close to 1:2:4 (Scheme 3) produced the complexes $[HQ]_2[Pb(Cl\text{-}pspa)_2]$ and $[HQ]_2[Pb(Br\text{-}pspa)_2]$. The formation of these compounds implies the requirement for an excess of Q with respect to the stoichiometric relationship (1:2:4 instead of 1:2:2). This probably ensures complete deprotonation of H_2(X-pspa) and facilitates the formation of the anionic complex. The other H_2(X-pspa) acids afforded unidentified solids, possibly mixtures of the 1:1 and 2:1:2 derivatives. $[HQ]_2[Pb(Cl\text{-}pspa)_2]$ and $[HQ]_2[Pb(Br\text{-}pspa)_2]$ are more soluble in DMSO and DMF than the corresponding 1:1 complexes, but they are insoluble in water and other common organic solvents and melt with decomposition at a rather high temperature (ca. 250 °C).

X-ray Diffraction

The single crystals of H_2(Cl-pspa) obtained by slow evaporation of the solvent from a solution of the compound in dichloromethane are composed of planar [root mean square (rms) deviation: 0.0232 Å] molecules (Figure 1). Selected bond lengths [Å] and angles [°] are listed in Table 1.

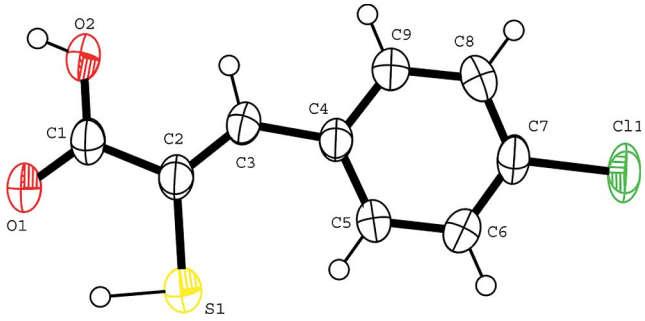

Figure 1. Molecular structure of H_2(Cl-pspa) with numbering scheme.

The S(1)–C(2) bond length [1.752(2) Å] is close to the sum of the covalent radii for the two atoms (1.78 Å)[16] and also to those found in the structurally related 3-(phenyl)- [1.749(3) Å][17] and 3-(2-chlorophenyl)-2-sulfanylpropenoic [1.766(7) Å][18] acids and 2-sulfanylbenzoic acid [1.766(3) Å].[19] The O(1)–C(1) and the O(2)–C(1) distances

 © 2013 Wiley-VCH Verlag GmbH & Co. KGaA, Weinheim

Table 1. Selected bond lengths [Å] and angles [°] in H_2(Cl-pspa) and $[HQ]_2[Pb(Cl\text{-}pspa)_2]$.

H_2(Cl-pspa)		$[HQ]_2[Pb(Cl\text{-}pspa)_2]$			
		Pb environment			
		Pb–S(1)	2.5899(16)		
		Pb–S(2)	2.6326(16)		
		Pb–O(11)	2.448(4)		
		Pb–O(21)	2.431(4)		
		S(1)–Pb–S(2)	99.04(5)		
		S(1)–Pb–O(11)	73.52(10)		
		S(1)–Pb–O(21)	76.60(10)		
		S(2)–Pb–O(11)	90.90(10)		
		S(2)–Pb–O(21)	72.51(9)		
		O(11)–Pb–O(21)	142.88(14)		
		Ligand 1		Ligand 2	
O(1)–C(1)	1.227(3)	O(11)–C(1)	1.281(7)	O(21)–C(10)	1.270(7)
O(2)–C(1)	1.305(3)	O(12)–C(1)	1.239(7)	O(22)–C(10)	1.242(7)
S(1)–C(2)	1.752(2)	S(1)–C(2)	1.743(6)	S(2)–C(11)	1.759(6)
C(1)–C(2)	1.483(3)	C(1)–C(2)	1.536(8)	C(10)–C(11)	1.515(8)
C(2)–C(3)	1.345(3)	C(2)–C(3)	1.350(8)	C(11)–C(12)	1.338(8)
C(3)–C(4)	1.464(3)	C(3)–C(4)	1.460(8)	C(12)–C(13)	1.461(8)
O(1)–C(1)–O(2)	122.6(2)	O(11)–C(1)–O(12)	124.2(5)	O(21)–C(10)–O(22)	121.7(5)
O(1)–C(1)–C(2)	122.2(2)	O(11)–C(1)–C(2)	117.9(5)	O(21)–C(10)–C(11)	119.6(5)
O(2)–C(1)–C(2)	115.2(2)	O(12)–C(1)–C(2)	117.9(5)	O(22)–C(10)–C(11)	118.7(5)
S(1)–C(2)–C(3)	124.94(19)	S(1)–C(2)–C(3)	124.9(5)	S(2)–C(11)–C(12)	125.4(5)
C(1)–C(2)–C(3)	119.6(2)	C(1)–C(2)–C(3)	116.4(5)	C(10)–C(11)–C(12)	117.0(5)
C(2)–C(3)–C(4)	131.5(2)	C(2)–C(3)–C(4)	131.2(6)	C(11)–C(12)–C(13)	132.4(6)

are in the ranges 1.21–1.25 and 1.31–1.35 Å, which fall within the ranges suggested[20] to define C=O(1) and a C–O(2) bonds in ordered carboxylic acid dimers supported by O–H···O bonds, as was found in this case (Table 2).

Table 2. Structural parameters [Å and °] describing intra- and intermolecular hydrogen bonding in [H_2(Cl-pspa)] and $[HQ]_2[Pb(Cl\text{-}pspa)_2]$.

D–H···A	*d*(D–H)	*d*(H···A)	*d*(D···A)	∠DHA
[H_2(Cl-pspa)]				
S(1)–H(1S)···O(1)	1.29(4)	2.07(4)	2.9416(19)	120(2)
O(2)–H(1O)···O(1)[a]	0.77(4)	1.88(4)	2.649(3)	172(4)
S(1)–H(1S)···Cl(1)[b]	1.29(4)	2.91(4)	3.7587(12)	122(2)
$[HQ]_2[Pb(Cl\text{-}pspa)_2]$				
N(2)–H(2B)···O(11)	0.92	1.95	2.867(6)	177.8
N(1)–H(1A)···O(12)	0.92	1.86	2.764(6)	168.1
N(1)–H(1B)···O(21)[c]	0.92	1.97	2.865(6)	164.6
N(1)–H(1B)···O(22)[c]	0.92	2.38	3.101(6)	135.0
N(2)–H(2A)···O(22)[c]	0.92	1.80	2.718(6)	172.9

[a] Symmetry code: $-x + 2, -y, -z + 1$. [b] $x - 1, y - 1, z$. [c] $x, y + 1, z$.

In addition to the O–H···O hydrogen bonds that link the molecules into dimers, other intra- and intermolecular interactions are present in H_2(Cl-pspa). An intramolecular S–H···O bond (Table 2), also detected in the two previously cited[17,18] and similar sulfanylpropenoic acids but absent in 2-sulfanylbenzoic acid,[19] is present in this case. Furthermore, the S–H group and the Cl atom of a neighbouring molecule are involved in an S–H···Cl hydrogen bond (Table 2) that links the dimers into sheets. In these sheets, the Cl atom is located 3.296 Å from another Cl atom of a neighbouring molecule (a smaller distance than the sum of the van der Waals radii, 3.50 Å);[21] additionally, the Cl atom is 3.404 Å from C(1) of a molecule of a parallel sheet.

The structures of $[HQ]_2[Pb(Cl\text{-}pspa)_2]$ and $[HQ]_2[Pb(Br\text{-}pspa)_2]$ are isotypic, so only the chloro derivative will be discussed {the data for the $[HQ]_2[Pb(Br\text{-}pspa)_2]$ complex are given in Tables S1 and S2 and Figure S1}. A representation of the $[Pb(Cl\text{-}pspa)_2]^{2-}$ anion is displayed in Figure 2 (a). Selected bond lengths and angles are given in Table 1. The lattice consists of $[Pb(Cl\text{-}pspa)_2]^{2-}$ anions and $[HQ]^{2+}$ cations. In the former, the Pb^{II} ions are O,S-chelated by two fully deprotonated sulfanylpropenoate ligands to give a coordination number of four. The distribution of the Pb–O and Pb–S bonds on one side of the Pb^{II} ion suggest the presence of a stereochemically active lone pair (SALEP) projected out in the opposite direction. This hemidirected coordination sphere[22] can be described as a pseudo-trigonal bipyramid in which the two O atoms are apical and the two S atoms plus the SALEP are in the equatorial positions. A similar kernel was depicted for some neutral Pb^{II} complexes with thiomaltol,[11] 3-hydroxy-1,2-dimethyl-4(1*H*)-pyridinethione[11] and thiohydroxamic acids.[23] As expected, the Pb–O bond lengths are shorter than those in other Pb^{II} complexes with stereochemically active lone pairs, but with higher coordination numbers.[24]

The main distortion in this pseudo-trigonal-bipyramidal arrangement is associated with the bond angles O(11)–Pb–O(21) and S(1)–Pb–S(2), which are narrower [142.88(14) and 99.04(5)°, respectively] than the ideal values (180 and 120°). In addition, the O(11)–Pb–S(1), O(21)–Pb–S(1) and O(21)–Pb–S(2) angles are smaller (73–77°) than the ideal angle (90°), although O(11)–Pb–S(2) is close to this value [90.90(10)°]. As revealed previously,[23] these deviations from the canonical geometry could be due to the influence of the SALEP, which repels and compresses the bonding

 © 2013 Wiley-VCH Verlag GmbH & Co. KGaA, Weinheim

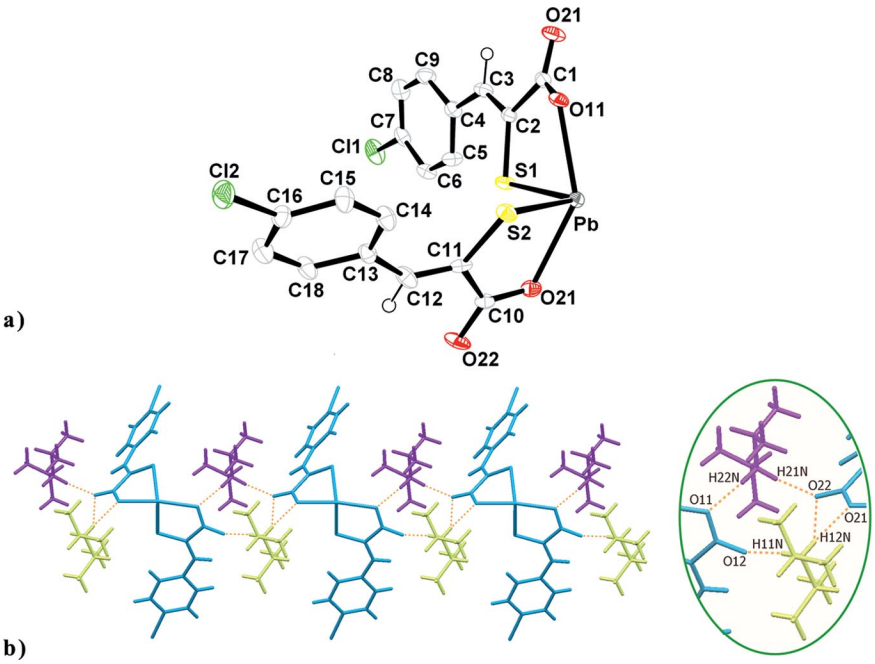

Figure 2. (a) Structure of $[Pb(Cl\text{-}pspa)_2]^{2-}$ anion with numbering scheme. (b) View of the hydrogen-bonded chain formed between HQ^+ cations and $[Pb(Cl\text{-}pspa)_2]^{2-}$ anions.

pairs, but also the small bite of the ligand, which conditions the O(11)–Pb–S(1) and O(21)–Pb–S(2) angles. These angles [73.52(10) and 72.51(9)°, respectively] are practically equal to those found in $[PbPh_2(pspa)_2]^{2-}$ [73.51(12) and 71.23(11)°],[14] an anionic complex with a ligand similar to Cl-pspa^{2-} but without a SALEP as the complex is a Pb^{IV} derivative. It is worth comparing the Pb–O and Pb–S bond lengths in the $[Pb(Cl\text{-}pspa)_2]^{2-}$ and $[PbPh_2(pspa)_2]^{2-}$ complexes. In the Pb^{II} compound, the Pb–O distances are shorter [2.431(4) and 2.448(4) Å] than those in the diphenyllead(IV) complex [2.480(5) and 2.569(5) Å], whereas the Pb–S distances remain practically unchanged [2.5899(16), 2.6326(16) and 2.5975(19), 2.6198(19) Å, respectively]. This suggests that Pb^{II} ions are possibly "harder" than $PbPh_2^{2+}$, although the former is a borderline Lewis acid.[25]

The bond lengths and angles of the ligand change only marginally upon deprotonation and coordination. The main modification occurs in the length of the two carboxylate C–O bonds, which became more similar in the complex (Table 1). Moreover, the two ligands $[Cl\text{-}pspaS(1)]^{2-}$ and $[Cl\text{-}pspaS(2)]^{2-}$ are not equivalent and differ mainly in their respective planarity, which is reduced in both cases with respect to that of the free ligand (vide supra). The dihedral angle between the two fragments that are approximately planar in their backbones, namely, the phenyl ring and the sulfanylpropenoate moieties, is 23.35(19) for $[Cl\text{-}pspaS(1)]^{2-}$ and 18.66(24)° for $[Cl\text{-}pspaS(2)]^{2-}$.

The $[Pb(Cl\text{-}pspa)_2]^{2-}$ complex anions are associated in the lattice through hydrogen bonds, in which two types of diisopropylammonium cations participate; this results in chains along the *b* axis (Figure 2, b). The HQ^+ cation containing N(1) forms a bifurcated donor hydrogen bond involving N–H(1A) and the two carboxylate O atoms from a neighbouring ligand. In one of these bonds [N–H(1A)···O(22)], the distance is larger, and the DHA angle is narrower than in the other [N–H(1A)···O(21), see Table 2]. However, despite this difference, they are within the usual range for this type of bond.[26] The same HQ^+ cation forms an additional bond [N(1)–H(1B)··O(12)] with another ligand and, thereby, contributes to connect the $[Pb(Cl\text{-}pspa)_2]^{2-}$ anions. The HQ^+ cation containing N(2) forms only two bridging hydrogen bonds and these also contribute to the catenation.

In contrast to the situation in the complexes of the thiohydroxamic acids,[23] in $[Pb(Cl\text{-}pspa)_2]^{2-}$ there are no significant additional bonds with the metal ion. In the crystal (Figure 3, a), the closest atoms to the Pb^{II} ion, other than those of the coordination sphere, are three H atoms belonging to a phenyl ring [Pb···H(18) 3.198 Å, symmetry code *x*, 3/2 – *y*, 1/2 + *z*] and to two diisopropylammonium methyl groups [Pb···H(42B) 3.208 Å, symmetry code *x*, 1/2 – *y*, 1/2 + *z*; Pb···H(50C) 3.427 Å, symmetry code *x*, 1 + *y*, *z*; Figure 3, b]. Although the formation of some agostic interactions between the SALEP and H–C bonds was considered,[27] it would be expected that, if such interactions occur, they would be located over the gap where the stereochemical lone pair is believed to reside and, in the present complex, this is not the case (see magnified view in Figure 3, b).

There is also one Cl atom (symmetry code –1 – *x*, 1 – *y*, –*z*) located 3.896 Å from the metal centre. Although in this case a secondary interaction with Pb^{II} is plausible, this distance is a little higher than the sum of the van der Waals radii of the two atoms (2.00 and 1.75 Å for Pb[10] and Cl,[21] respectively).

 © 2013 Wiley-VCH Verlag GmbH & Co. KGaA, Weinheim

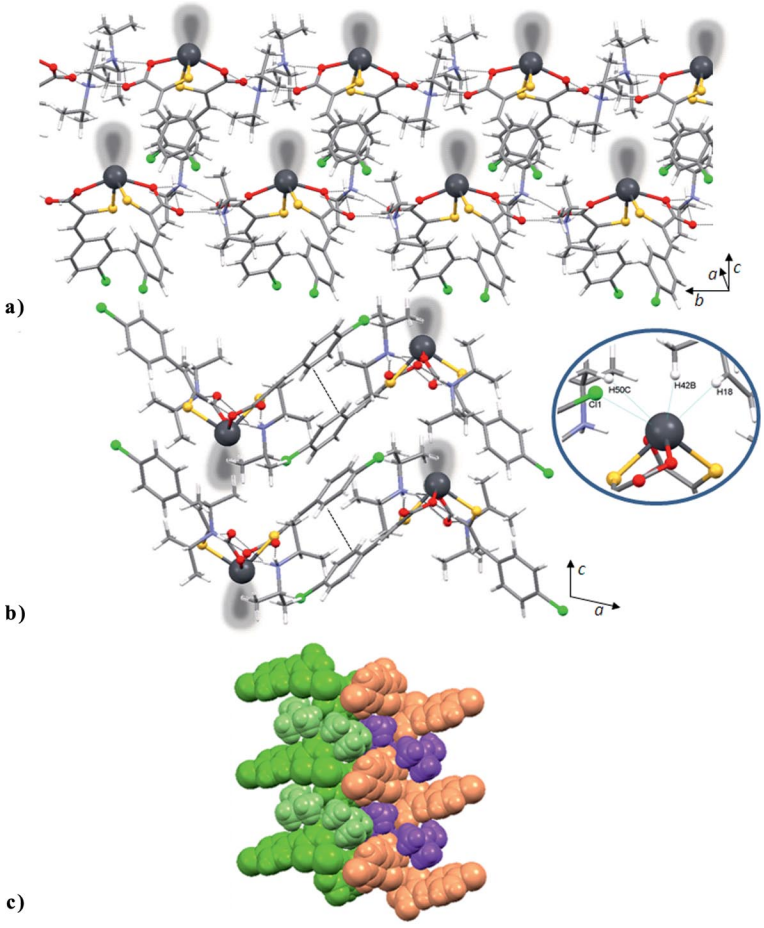

Figure 3. (a) Packing of the chains in the lattice of $[HQ]_2[Pb(Cl\text{-}pspa)_2]$ along the *b* axis showing the SALEPs. (b) A view of the chains along the *a* axis showing the π-stacking interactions and, in the enlarged detail, the unbound atoms closest to Pb^{II}. (c) View of the packing in $[HQ]_2[Pb(Cl\text{-}pspa)_2]$. The HQ^+ cations are in light yellow and cyan, and the two ligands of the $[Pb(Cl\text{-}pspa)_2]^{2-}$ anions are in brown and green.

The chains are held in pairs by π-stacking interactions between the phenyl rings [C(5)···C(5)^d 3.312 Å, symmetry code 1 – *x*, –*y*, 1 – *z*], which are in a slipped alignment.[28] The tapes thus formed pack together in the lattice without any relevant additional interactions.

A visual analysis of Figure 3 (a and b) suggests that the packing mode of $[HQ]_2[Pb(Cl\text{-}pspa)_2]$ is somehow arranged to provide enough space to avoid destabilizing interactions involving the SALEP. The resulting packing efficiency is very good (see Figure 3, c) according to the Kitaigorodskii packing index[29] (68 % for the Cl-pspa^{2-} derivative and 69 % in the Br-pspa^{2-} complex) calculated by using the CALC VOID routine of PLATON.[30]

Spectroscopy Studies

The IR spectra of the H_2(X-pspa) ligands show a ν(S–H) band in the range 2590–2560 cm^{-1}. The bands of the vibrations of the –COOH groups [ν(C=O), δ(OH) and ν(C–O)] are in the ranges 1730–1680, 1440–1395 and 1320–1210 cm^{-1}, respectively.

The two classes of complexes described in this paper, [Pb(X-pspa)] and $[HQ]_2[Pb(X\text{-}pspa)_2]$, have a common feature in the IR spectra and this is the absence of the ν(S–H) band, which is consistent with the deprotonation of the S–H group in all cases. In addition, the characteristic bands of the COOH group are replaced by the two typical bands of the carboxylate group [$\nu_{as}(CO_2^-)$ and $\nu_{sym}(CO_2^-)$], a finding consistent with the deprotonation of the COOH group.

Only for the second class of compounds was it possible to study some examples by X-ray diffraction. This study shows (vide supra) that in $[HQ]_2[Pb(Cl\text{-}pspa)_2]$ and $[HQ]_2[Pb(Br\text{-}pspa)_2]$ the carboxylate group of the ligand acts in a monodentate manner and is hydrogen bonded to the N–H group of the diisopropylammonium cation. The IR spectra of both compounds show the carboxylate bands at 1520/1317 (Cl) and 1522/1315 cm^{-1} (Br) and, thus, give values of 203 and 207, respectively, for the parameter Δν [$\nu_{as}(CO_2^-) - \nu_{sym}(CO_2^-)$]. These values are close to those found previously in similar complexes[13,14,31] and, bearing in mind the effect of the hydrogen bond,[32] fall inside the general range for monodentate carboxylate groups.[33] The lower value found for the F derivative, 188, can be attributed to the presence in the lattice of a stronger hydrogen bond, though the participation of the carboxylate group in some additional interaction cannot be ruled out.

 © 2013 Wiley-VCH Verlag GmbH & Co. KGaA, Weinheim

The positions of the $\nu_{as}(CO_2^-)$ and $\nu_{sym}(CO_2^-)$ bands in the [Pb(X-pspa)] complexes led to values of 166–199 for the parameter $\Delta\nu$. These values fall inside the general range[33] for bridging carboxylate groups. However, it should be noted that for this specific class of sulfanylpropenoate ligands, we have previously found values within this range for the bridging coordination mode[14,34] or bidentate and bridge[35] mode of the carboxylate group. Therefore, both coordination modes would be compatible with the experimental IR data for this class of compound.

The mass spectra of the ligand and complexes were recorded by using FAB or ESI-TOF ionization methods (see Experimental Section). Owing to its soft character, ESI-MS is a good approach to explore the species present in the solutions of a coordination compound.[36,37] The ESI-MS data for [Pb(X-pspa)] and $[HQ]_2[Pb(X\text{-}pspa)_2]$ (X = Cl, Br) in DMSO solution will be discussed as representative examples of the 1:1 and 1:2 derivatives prepared in this study.

In the positive ESI spectra of the [Pb(X-pspa)] complexes, the dominant metallated ion is $[Pb(X\text{-}pspa) + H]^+$ and this confirms the permanence of the Pb^{II}–$pspa^{2-}$ coordination even in the presence of a donor solvent such as DMSO. Other subsidiary peaks appear in the spectra, and these correspond to metallated ions that in some cases contain DMSO. Notably, once in solution, it can be expected that the limited coordination sphere of the Pb^{II} ion will increase, probably by incorporation of DMSO molecules instead of the intermolecular interactions described in the solid state. However, the negative-ion-mode experiments suggest that not all [Pb(X-pspa)] molecules remain unchanged in the gas phase because some ions derived from $X\text{-}pspa^{2-}$ and their disulfide, such as $[X\text{-}pspa + H]^-$ and $[X\text{-}pspa\text{-}S\text{–}S\text{-}pspa\text{–}X]^{2-}$, appear in these spectra. The latter species contain S–S bonds and these can be formed by oxidation of $X\text{-}pspa^{2-}$ during the ionization process or in DMSO solution (vide infra).

The ESI(+) MS data for $[HQ]_2[Pb(X\text{-}pspa)_2]$ show weak signals for the $[Pb(X\text{-}pspa)_2 + 3H]^+$ ions but the base peaks correspond to the protonated 1:1 derivative, which suggests a partial dissociation of the 1:2 complexes in the course of dissolution and/or ionization. The spectra in the negative mode give complementary information in this respect. Although the signals corresponding to nonmetallated oxidized species are again predominant, several metallated monoanions such as $[Pb(X\text{-}pspa)_2 + H]^-$ (Figure 4) are significantly abundant; therefore, the total dissociation of $[Pb(X\text{-}pspa)_2]^{2-}$ in the dissolution/ionization processes can be excluded.

The NMR signals (see Experimental Section) were assigned by considering previous data for rhodanines,[38] sulfanylpropenoic acids[34,35] and complexes,[13,14,34,39] and on the basis of gradient heteronuclear multiple quantum coherence (gHMQC) and gHMBC experiments when necessary. Freshly prepared solutions of $[D_6]$DMSO were used to record the spectra, but even under these conditions H_2(I-pspa) evolved very rapidly to give new species (possibly the disulfide), which were not fully characterized. In these cases, the use of $[D_4]$methanol as an alternative solvent was necessary.

In the ^1H NMR spectra, the benzylidene rhodanines show a broad singlet at $\delta \approx 14$ ppm, assigned to the –NH group. The large deshielding of this signal could be explained by the persistence in solution of the hydrogen bond found in the solid state.[38] The benzylidene rhodanines also show a signal at $\delta \approx 7.5$ ppm, which corresponds to the –CH= group, and signals between $\delta = 8$ and 7 ppm from the aromatic protons. The –OH proton of HOp-Rhod was observed as a broad singlet at $\delta = 10.4$ ppm.

The spectra of the H_2(X-pspa) ligands show a very broad lowfield signal at $\delta \approx 13$ ppm, assigned to the proton of the –COOH group, and a broad peak at $\delta \approx 5$ ppm attributed to the SH proton. For H_2(HO-pspa), a broad singlet was observed at $\delta = 9.48$ ppm, and this is assigned to the phenol proton.

The [Pb(X-pspa)] and $[HQ]_2[Pb(X\text{-}pspa)_2]$ complexes are more stable than the ligands in DMSO solution, and insignificant amounts of decomposition products were observed during the time necessary to record the spectra. The presence of the $[X\text{-}pspa\text{-}S\text{–}S\text{-}pspa\text{-}X]^{2-}$ anions is easily detected by analyzing the position of the C(3)–H signal, which appears at lower field for the disulfides than in the free ligand, and in the complexes it appears at higher field (vide infra). Accordingly, it must be concluded that the oxidized species observed in the ESI-MS measurements are derived from desorption and the ionization process in the gas phase, despite the soft character of ESI. The possible partial dissociation of $[Pb(X\text{-}pspa)_2]^{2-}$ in DMSO solution cannot be conclusively established. There is no duplicity of signals, including those of the free anions, but this could be the case if free and coordinated $(X\text{-}pspa)^{2-}$ anions interchange very rapidly. However, the very sharp signals observed in the spectra are not consistent with an interchange process.

The spectra of [Pb(X-pspa)] and $[HQ]_2[Pb(X\text{-}pspa)_2]$ were compared with those of the corresponding ligand. The spectra of the complexes lack the signals at $\delta \approx 5$ and 13 ppm, which clearly shows that the ligand is bideprotonated; furthermore, the C(3)–H signal is located at higher field that in the corresponding ligand, which indicates that the S coordination observed in the solid state remains in solution.[39] The spectrum of [Pb(HO-pspa)] contains the signal of the –OH substituent, and this shows that this group is not deprotonated. Integration of the $[HQ]_2[Pb(X\text{-}pspa)_2]$ spectra is consistent with the proposed stoichiometry in the solid state and the location of the ligand signals, which are sensitive to metallation, in similar positions to those of the corresponding [Pb(X-pspa)] compounds discussed above also suggest an O,S coordination mode for the ligands. A septuplet and a doublet at high field in the spectra were assigned to the –C(H) and CH_3 groups of the diisopropylammonium cation, and the very broad signal at $\delta \approx 8$ ppm was ascribed to the NH_2^+ moiety of $[HQ]^+$.

As could be expected, in the ^{13}C NMR spectra of the ligands an important dependence of the position of the C(7) signal on the nature of the *para*-X atom was observed. In the complexes, the S coordination was confirmed by the

 © 2013 Wiley-VCH Verlag GmbH & Co. KGaA, Weinheim

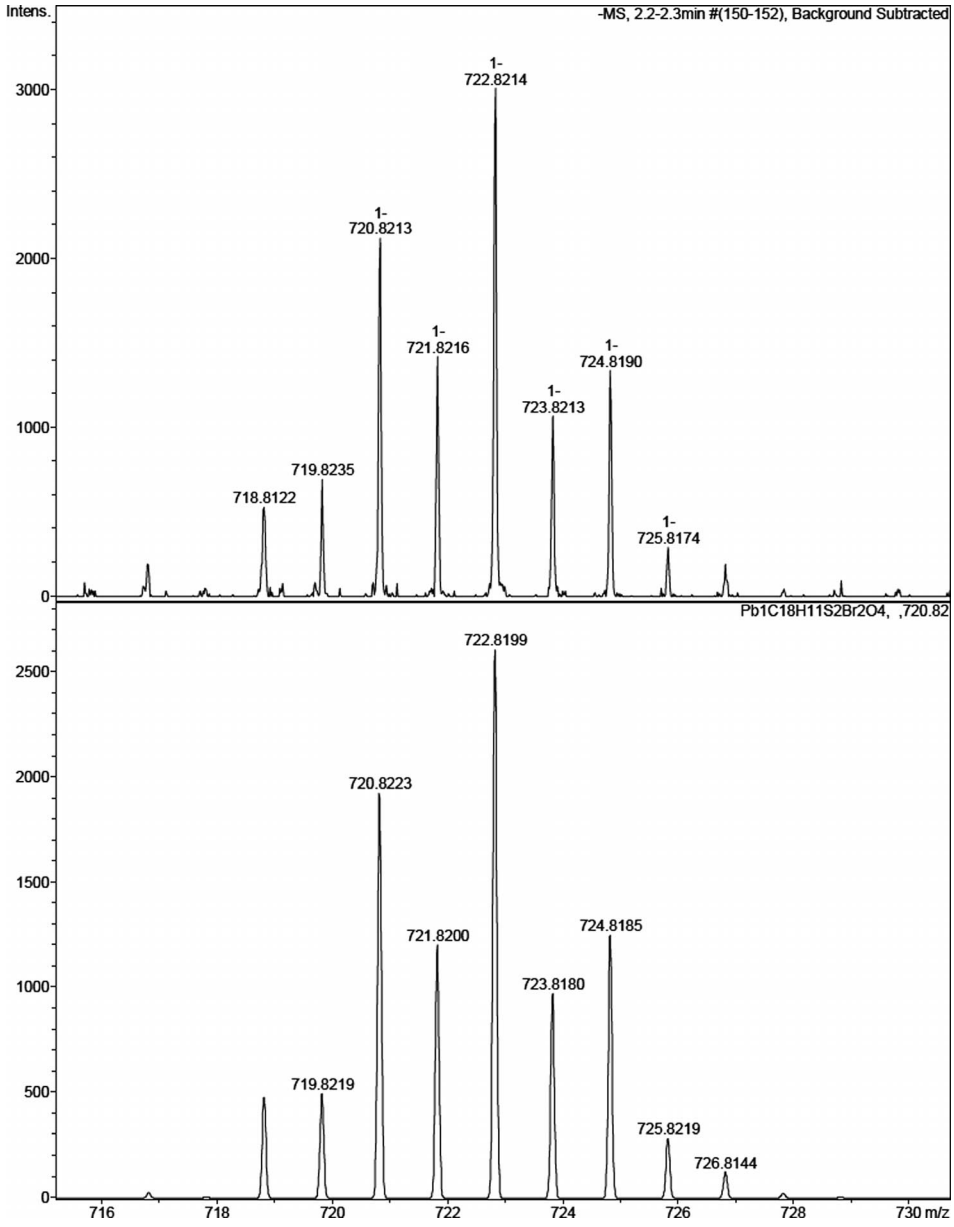

Figure 4. Comparison of the $[Pb(Br\text{-}pspa)_2 + H]^-$ signals in the experimental (upper trace) and simulated (lower trace) ESI(–) MS spectra of $[HQ]_2[Pb(Br\text{-}pspa)_2]$.

large deshielding of C(2) with respect to the corresponding ligands,[13,14,34,39] and the large downfield shift of C(1) provided evidence for the coordination of the carboxylate group.

Conclusions

The H_2(X-pspa) acids readily coordinate to the Pb^{II} ion in ethanol/water to give 1:1 [Pb(X-pspa)] complexes. When the reactions were performed in the presence of an excess of diisopropylamine (Q), which facilitates the deprotonation of the acids and can assume the role of counterion once protonated, 1:2 $[HQ]_2[Pb(X\text{-}pspa)_2]$ complexes were isolated (X = –Cl and –Br).

According to the results of IR studies, in the solid 1:1 complexes the Pb^{II} ion is coordinated to the ligand through the deprotonated sulfhydryl and carboxylate groups, and the latter possibly form bridges between two metal centres to give a polymeric arrangement. The NMR and ESI-MS evidence indicate that the ligand remains coordinated to the Pb^{II} centre in DMSO solution. In the gas phase, desorption and ionization under ESI-MS conditions favours the partial dissociation and oxidation of the ligand. These two phenomena were not observed in solution, even after several weeks.

The complexes with $[HQ]_2[Pb(X\text{-}pspa)_2]$ stoichiometry consist of $[Pb(X\text{-}pspa)_2]^{2-}$ anions connected in chains through hydrogen bonding with the $[HQ]^+$ anions. The

 © 2013 Wiley-VCH Verlag GmbH & Co. KGaA, Weinheim

anions contain two O,S-bonded ligands, and the distribution of the Pb–O and Pb–S bonds on one side of the Pb^{II} ion suggest the presence of a stereochemically active lone pair. The chains are held in pairs by π-stacking interactions and arrange in a very efficient packing mode, which seems to be adopted to provide enough space around the lone pair to avoid repulsive interactions. Thus, these complexes provide an interesting example of the relevance of the lone pair in the supramolecular structures of Pb^{II} derivatives. ESI-MS and NMR studies were not conclusive regarding the partial dissociation of $[Pb(X\text{-pspa})_2]^{2-}$ in DMSO solution. The ESI-MS data show that this partial dissociation occurs in the gas phase, but the NMR measurements did not provide any evidence of this process; this suggests that the dissociated species in the mass spectra are formed during the desorption and ionization processes.

The stability of the complexes in solution, even in the presence of donor solvents, supports the possibility that H_2(X-pspa) can efficiently capture Pb^{II} ions in biological media and reduce its lethal effects. Although the simple complexes prepared in the present work are not soluble in aqueous media, they could evolve in vivo to more hydrosoluble mixed species with natural ligands, which could be susceptible to urinary excretion. These species could also be decorporated from the liver into the faeces by bile by taking advantage of the lipophilic character of the aromatic ring. Some previous evidence for the antidotic action of sulfanylpropenoic acids against Pb^{II} toxicity in rodents has been published.[40]

Experimental Section

Material and Methods

Elemental analyses were performed with a Carlo Erba 1108 microanalyzer. Melting points were determined with a Büchi apparatus. Mass spectra were recorded by using FAB (Micro mass Autospec spectrometer connected to a DS90 system, *m*-nitrobenzyl alcohol, Xe, 8 eV; ca. 1.28×10^{-15} J) and ESI-TOF (positive and negative-ion mode, Microtof® from Bruker Daltonics, DMSO, capillary voltage 4.5 kV) ionization methods. IR spectra (from KBr pellets or Nujol mulls) were recorded with a Bruker IFS66V FTIR spectrometer and are reported in the synthesis section with the following abbreviations: vs = very strong, s = strong, m = medium, w = weak, sh = shoulder, br. = broad. ^1H and ^{13}C NMR spectra were recorded at room temperature with a Bruker DPX 250 spectrometer operating at 250.13 MHz, a Varian Mercury-300 or a Varian Inova 400 system operating at 399.97 and 100.58 MHz or a Varian Inova 500 spectrometer operating at 500.14 and 125.76 MHz with 5 mm o.d. tubes in $[D_6]$DMSO or $[D_4]$MeOD. Chemical shifts are reported relative to tetramethylsilane (TMS) by using the solvent signal (δ^1H = 2.50 ppm, $\delta^{13}C$ = 39.5 ppm and δ^1H = 3.31 ppm, $\delta^{13}C$ = 49.00 ppm for DMSO and methanol, respectively) as reference. The signals are described as follows: chemical shift, multiplicity (s = singlet, d = doublet, dd = doublet of doublets, t = triplet, pst = pseudotriplet, q = quadruplet, sept = septuplet, br. = broad, vbr. = very broad). See Scheme 2 for atom numbering scheme. The low solubility of the compounds precluded ^{207}Pb NMR experiments.

Rhodanine, 4-fluorobenzaldehyde, 4-chlorobenzaldehyde, 4-bromobenzaldehyde, 4-iodobenzaldehyde and 4-trifluoromethoxybenzaldehyde were used as supplied by Aldrich. The benzylidene rhodanines used as precursors for the sulfanylpropenoic acids [5-(4-fluorobenzylidene)rhodanine (Fp-Rhod), 5-(4-chlorobenzylidene)rhodanine (Clp-Rhod), 5-(4-bromobenzylidene)rhodanine (Brp-Rhod), 5-(4-iodobenzylidene)rhodanine (Clp-Rhod) and 5-(4-trifluoromethoxybenzylidene)rhodanine (F_3COp-Rhod)] were prepared by condensation of rhodanine with the appropriate aldehyde (Scheme 4).[41] Rhodanine (0.02 mol in 40 mL of 0.4 M NaOH) was added to the appropriate aldehyde in a solution of acetic acid (10 mL) and ethanol (20 mL). After stirring of the mixture at 60–80 °C for 30 min, the resulting solid was collected by filtration and vacuum dried. The synthesis and characterization of [5-(4-hydroxybenzylidene)rhodanine (HOp-Rhod) and 5-(4-methoxybenzylidene)rhodanine (CH_3Op-Rhod) were described previously.[38]

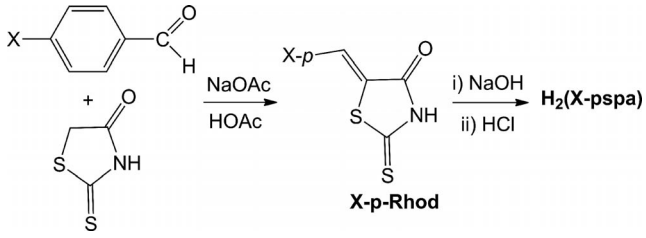

Scheme 4.

Fp-Rhod: Yellow solid, yield 85%, m.p. 215 °C. $C_{10}H_6FNOS_2$ (239.29): calcd. C 50.20, H 2.53, N 5.85, S 26.80; found C 49.94, H 2.52, N 5.88, S 25.98. ^1H NMR ($[D_6]$DMSO): δ = 7.42 (s, 1 H), 7.64 (pst, 2 H), 7.36 (pst, 2 H), 13.85 (br s, 1 H) ppm.

Clp-Rhod: Yellow solid, yield 94%, m.p. 225 °C. $C_{10}H_6ClNOS_2$ (255.75): calcd. C 46.97, H 2.36, N 5.48, S 25.07; found C 46.47, H 2.26, N 5.46, S 25.57. ^1H NMR ($[D_6]$DMSO): δ = 7.63 (s, 1 H), 7.61 (d, 2 H), 7.61 (d, 2 H), 13.75 (br s, 1 H) ppm.

Brp-Rhod: Yellow solid, yield 82%, m.p. 234 °C. $C_{10}H_6BrNOS_2$ (300.20): calcd. C 40.01, H 2.01, N 4.67, S 21.36; found C 39.92, H 1.78, N 4.68, S 21.32. ^1H NMR ($[D_6]$DMSO): δ = 7.61 (s, 1 H), 7.73 (d, 2 H), 7.53 (d, 2 H), 13.87 (br s, 1 H) ppm.

Ip-Rhod: Yellow solid, yield 85%, m.p. 245 °C. $C_{10}H_6INOS_2$ (347.20): calcd. C 34.60, H 1.74, N 4.03, S 18.47; found C 34.68, H 1.72, N 4.04, S 18.39. ^1H NMR ($[D_6]$DMSO): δ = 7.56 (s, 1 H), 7.89 (d, 2 H), 7.35 (d, 2 H), 13.86 (br s, 1 H) ppm.

F_3COp-Rhod: Yellow solid, yield 95%, m.p. 170 °C. $C_{11}H_6F_3NO_2S_2$ (305.30): calcd. C 43.28, H 1.98, N 4.59, S 21.00; found C 43.01, H 1.90, N 4.59, S 21.55. ^1H NMR ($[D_6]$DMSO): δ = 7.61 (s, 1 H), 7.57 (d, 2 H), 7.10 (d, 2 H), 13.77 (br s, 1 H) ppm.

Synthesis of Ligands: 3-(2-Aryl)-2-sulfanylpropenoic acids [H_2(X-pspa)] were prepared by hydrolysis of the appropriate benzylidene rhodanine precursor (10^{-2} mol) in an alkaline medium (50 mL of 1 M NaOH) (Scheme 4). After stirring under reflux for 30 min, the solution was cooled and neutralized with 1 M HCl. The resulting solid was collected by filtration and vacuum dried. The synthesis and characterization of H_2(CH_3O-pspa) were described previously.[32]

H_2(F-pspa): Beige solid, yield 63%. Mp 115 °C. $C_9H_7FO_2S$ (198.22): calcd. C 54.54, H 3.56, S 16.17; found C 54.88, H 3.19, S 16.82. MS (EI): *m*/*z* (%) = 197 (77) $[M - H]^+$, 153 (100) $[M - COOH]^+$. IR (KBr): $\tilde{\nu}$ = 1668 [vs, ν(C=O)], 1421 [s, δ(OH)], 1234 [vs, ν(C–O)], 2577 [s, ν(S–H)] cm^{-1}. ^1H NMR ($[D_6]$DMSO): δ = 13.35 (vbr. s, 1 H, 1-OH), 5.34 (vbr. s, 1 H, 2-H), 7.73 (s, 1 H, 3-H), 7.73 (dd, $^3J_{^1H,^1H}$ = 7.7, $^3J_{^1H,^{19}F}$ = 5.8 Hz, 2 H, 5-H and 9-H), 7.31 (pst, $^3J_{^1H,^1H}$ = 7.8, $^3J_{^1H,^{19}F}$ = 7.8 Hz, 2 H, 6-H and 8-H) ppm.

© 2013 Wiley-VCH Verlag GmbH & Co. KGaA, Weinheim

^{13}C NMR ([D$_6$]DMSO): δ = 166.3 (C-1), 124.0 (C-2), 132.5 (C-3), 131.5 (d, $^4J_{^{13}C,^{19}F}$ = 2.46 Hz, C-4], 132.0 (d, $^3J_{^{13}C,^{19}F}$ = 8.4 Hz, C-5, C-9), 115.8 (d, $^2J_{^{13}C,^{19}F}$ = 21.66 Hz, C-6, C-8), 161.9 (d, $^1J_{^{1}C,^{19}F}$ = 248.3 Hz, C-7] ppm.

H$_2$(Cl-pspa): Beige solid, yield 43%. Mp 175 °C. $C_9H_7ClO_2S$ (214.67): calcd. C 50.36, H 3.29, S 14.93; found C 50.18, H 3.11, S 14.96. MS (EI): *m/z* (%) = 213 (88) [M – H]$^+$, 169 (100) [M – COOH]$^+$. IR (KBr): $\tilde{\nu}$ = 1684 [vs, ν(C=O)], 1421 [s, δ(OH)], 1258 [vs, ν(C–O)], 2571 [s, ν(S–H)] cm^{-1}. ^{1}H NMR ([D$_6$]DMSO): δ = 13.29 (v br. s, 1 H, 1-OH), 5.41 (v br. s, 1 H, 2-H), 7.71 (s, 1 H, 3-H), 7.69 (d, 2 H, 5-H and 9-H), 7.54 (d, 2 H, 6-H and 8-H) ppm. ^{13}C NMR ([D$_6$]DMSO): δ = 166.2 (C-1), 125.3 (C-2), 132.1 (C-3), 133.3 (C-4), 131.4 (C-5 and C-9), 128.8 (C-6 and C-8), 133.8 (C-7) ppm. Single crystals were grown by slow evaporation of a dichloromethane solution.

H$_2$(Br-pspa): Beige solid, yield 58%. Mp 175 °C. $C_9H_7BrO_2S$ (259.12): calcd. C 41.72, H 2.72, S 12.37; found C 41.63, H 2.57, S 11.59. MS (EI): *m/z* (%) = 259 (100) [M – H]$^+$, 215 (70) [M – COOH]$^+$. IR (KBr): $\tilde{\nu}$ = 1681 [vs, ν(C=O)], 1416 [s, δ(OH)], 1269 [vs, ν(C–O)], 2561 [s, ν(S–H)] cm^{-1}. ^{1}H NMR ([D$_6$]DMSO): δ = 13.20 (v br. s, 1 H, 1-OH), 5.31 (v br. s, 1 H, 2-H), 7.78 (s, 1 H, 3-H), 7.65 (d, 2 H, 5-H and 9-H), 7.60 (d, 2,6-H and 8-H) ppm. ^{13}C NMR ([D$_6$]DMSO): δ = 166.1 (C-1), 125.4 (C-2), 132.1 (C-3), 134.0 (C-4), 131.6 (C-5 and C-9), 131.5 (C-6 and C-8), 122.0 (C-7) ppm.

H$_2$(I-pspa): Beige solid, yield 75%. Mp 160 °C. $C_9H_7IO_2S$ (306.12): calcd. C 35.31, H 2.30, S 10.47; found C 35.94, H 2.34, S 9.73. MS (EI): *m/z* (%) = 305 (100) [M – H]$^+$, 261 (100) [M – COOH]$^+$. IR (KBr): $\tilde{\nu}$ = 1676 [vs, ν(C=O)], 1414 [s, δ(OH)], 1256 [vs, ν(C–O)], 2559 [s, ν(S–H)] cm^{-1}. ^{1}H NMR ([D$_6$]DMSO): δ = 13.50 (v br. s, 1 H, 1-OH), 7.65 (s, 1 H, 3-H), 7.83 (d, 2 H, 5-H and 9-H), 7.46 (d, 2 H, 6-H and 8-H) ppm. ^{13}C NMR ([D$_4$]MeOD): δ = 167.9 (C-1), 126.3 (C-2), 134.1 (C-3), 136.2 (C-4), 138.9 (C-5 and C-9), 132.6 (C-6 and C-8), 95.4 (C-7) ppm.

H$_2$(F$_3$CO-pspa): Beige solid, yield 79%. Mp 102 °C. $C_{10}H_7F_3O_3S$ (264.22): calcd. C 45.46, H 2.67, S 12.13; found C 45.80, H 2.75, S 11.69. MS (EI): *m/z* (%) = 527 (8) [2M – H]$^+$, 263 (100) [M – H]$^+$, 247 (25) [M – OH]$^+$, 219 (89) [M – COOH]$^+$. IR (KBr): $\tilde{\nu}$ = 1668 [vs, ν(C=O)], 1425 [s, δ(OH)], 1254 [vs, ν(C–O)], 2584 [s, ν(S–H)] cm^{-1}. ^{1}H NMR ([D$_6$]DMSO): δ = 13.19 (v br. s, 1 H, 1-OH), 7.76 (s, 1 H, 3-H), 8.52 (d, 2 H, 5-H and 9-H), 7.79 (d, 2 H, 6-H and 8-H) ppm. ^{13}C NMR ([D$_6$]DMSO): δ = 166.3 (C-1), 125.8 (C-2), 132.0 (C-3), 134.3 (C-4), 131.7 (C-5 and C-9), 121.2 (C-6 and C-8), 148.1 (C-7), 116.1 (q, $^1J_{^{13}C,^{19}F}$ = 256.9 Hz, C-10) ppm.

H$_2$(HO-pspa): Brown solid, yield 54%. Mp 165 °C. $C_9H_8O_3S$ (196.23): calcd. C 55.09, H 4.11, S 16.34; found C 54.94, H 4.08, S 15.96. MS (EI): *m/z* (%) = 195 (100) [M – H]$^+$, 178 (3) [M – OH]$^+$, 150 (100) [M – COOH]$^+$. IR (KBr): $\tilde{\nu}$ = 1686 [vs, ν(C=O)], 1443 [vs, δ(OH)], 1256 [vs, ν(C–O)], 2580 [m, ν(S–H)] cm^{-1}. ^{1}H NMR ([D$_6$]DMSO): δ = 13.29 (v br. s, 1 H, 1-OH), 5.12 (v br. s, 1 H, 2-SH), 7.66 (s, 1 H, 3-H), 7.55 (d, 2 H, 5-H and 9-H), 6.86 (d, 2 H, 6-H and 8-H), 10.05 (br s, 1 H, 7-OH) ppm. ^{13}C NMR ([D$_6$]DMSO): δ = 169.9 (C-1), 118.9 (C-2), 125.7 (C-3), 134.0 (C-4), 131.8 (C-5 and C-9), 115.6 (C-6 and C-8), 158.4 (C-7) ppm.

Synthesis of Complexes: The [Pb(X-pspa)] complexes were prepared by the same general method: to a solution of lead(II) acetate trihydrate in water was added a solution of the appropriate sulfanylcarboxylic acid in ethanol until a 1:1 molar ratio was achieved. The mixture was stirred for several hours, and the resulting solid was separated by centrifugation and dried under vacuum. For example, a solution of H$_2$(F-pspa) (0.10 g, 0.51 mmol) in ethanol (10 mL) was added to a solution of lead(II) acetate trihydrate (0.19 g, 0.51 mmol) in water (20 mL). The reaction mixture was stirred for 3 h, and the resulting solid was isolated.

[Pb(F-pspa)]: Beige solid, yield 93%. $C_9H_5FO_2PbS$ (403.42): calcd. C 26.80, H 1.25, S 7.95; found C 26.29, H 1.14, S 7.41. MS (FAB): *m/z* (%) = 405 (30) [Pb(F-pspa) + H]$^+$. IR (KBr): $\tilde{\nu}$ = 1504 [vs, $\nu_a(CO_2^-)$], 1323 [s, $\nu_s(CO_2^-)$] cm^{-1}. ^{1}H NMR ([D$_6$]DMSO): δ = 7.53 (s, 1 H, 3-H), 8.07 (dd, 2 H, 5-H and 9-H), 7.17 (pst, 2 H, 6-H and 8-H) ppm. ^{13}C NMR ([D$_6$]DMSO): δ = 182.7 (C-1), 137.5 (C-2), 133.1 (C-3), 134.1 (C-4), 132.5 (d, $^3J_{^{13}C,^{19}F}$ = 8.4 Hz, C-5, C-9), 114.7 (d, $^2J_{^{13}C,^{19}F}$ = 21.6 Hz, C-6, C-8), 160.6 (d, $^1J_{^{13}C,^{19}F}$ = 248.3 Hz, C-7) ppm.

[Pb(Cl-pspa)]: Orange solid, yield 78%. $C_9H_5ClO_2PbS$ (419.87): calcd. C 25.75, H 1.20, S 7.64; found C 25.51, H 1.08, S 7.22. MS (FAB): *m/z* (%) = 421 (10) [Pb(Cl-pspa) + H]$^+$. MS (ESI+): *m/z* (%) = 840 (5) [Pb$_2$(Cl-pspa)$_2$ + H]$^+$, 710 (2) [Pb(Cl-pspa)$_2$ + DMSO + 3H]$^+$, 635 (5) [Pb(Cl-pspa)$_2$ + 3H]$^+$, 498 (2) [Pb(Cl-pspa) + DMSO + H]$^+$, 443 (4) [Pb(Cl-pspa) + Na]$^+$, 421 (100) [Pb(Cl-pspa) + H]$^+$. MS (ESI–): *m/z* (%) = 427 (5) [(Cl-pspa-S–S-pspa-Cl) + H]$^-$, 319 (12) [(Cl-pspa-S–S-pspa-Cl)–COOH–COSH + H]$^-$, 214 (40) [Cl-pspa + H]$^-$, 213 (84) [(Cl-pspa-S–S-pspa-Cl)]$^{2-}$, 197 (12) [Cl-pspa–OH + H]$^-$, 169 (100) [Cl-pspa–COO]$^-$. IR (KBr): $\tilde{\nu}$ = 1514 [vs, $\nu_a(CO_2^-)$], 1321 [vs, $\nu_s(CO_2^-)$] cm^{-1}. ^{1}H NMR ([D$_6$]-DMSO): δ = 7.45 (s, 1 H, 3-H), 8.00 (d, 2 H, 5-H and 9-H), 7.36 (d, 2 H, 6-H and 8-H) ppm. ^{13}C NMR ([D$_6$]DMSO): δ = 182.1 (C-1), 140.1 (C-2), 132.2 (C-3), 136.6 (C-4), 132.0 (C-5 and C-9), 127.7 (C-6 and C-8), 130.1 (C-7) ppm.

[Pb(Br-pspa)]: Orange solid, yield 67%. $C_9H_5BrO_2PbS$ (464.32): calcd. C 23.28, H 1.09, S 6.90; found C 23.72, H 0.96, S 6.51. MS (ESI+): *m/z* (%) = 929 (1) [Pb$_2$(Br-pspa)$_2$ + H]$^+$, 803 (31) [Pb(Br-pspa)$_2$ + DMSO + 3H]$^+$, 725 (28) [Pb(Br-pspa)$_2$ + 3H]$^+$, 541 (3) [Pb(Br-pspa) + DMSO + H]$^+$, 487 (3)[Pb(Br-pspa) + Na]$^+$, 465 (100) [Pb(Br-pspa) + H]$^+$. MS (ESI–): *m/z* (%) = 537 (2) [(Br-pspa-S–S-pspa-Br) + Na]$^-$, 515 (41) [(Br-pspa-S–S-pspa-Br) + H]$^-$, 258 (93), [Br-pspa + H]$^-$, 257 (100) [(Br-pspa-S–S-pspa-Br)]$^{2-}$, 242 (9) [Br-pspa–OH + H]$^-$, 213 (51) [Br-pspa–COO]$^-$. IR (KBr): $\tilde{\nu}$ = 1516 [vs, $\nu_a(CO_2^-)$], 1319 [vs, $\nu_s(CO_2^-)$] cm^{-1}. ^{1}H NMR ([D$_6$]DMSO): δ = 7.43 (s, 1 H, 3-H), 7.94 (d, 2 H, 5-H and 9-H), 7.49 (d, 2 H, 6-H and 8-H) ppm. ^{13}C NMR ([D$_6$]DMSO): δ = 182.1 (C-1), 140.3 (C-2), 132.2 (C-3), 136.9 (C-4), 132.3 (C-5 and C-9), 130.6 (C-6 and C-8), 118.7 (C-7) ppm.

[Pb(I-pspa)]: Orange solid, yield 77%. $C_9H_5IO_2PbS$ (511.32): calcd. C 21.14, H 0.99, S 6.27; found C 21.35, H 1.18, S 5.84. IR (KBr): $\tilde{\nu}$ = 1516 [vs, $\nu_a(CO_2^-)$], 1317 [vs, $\nu_s(CO_2^-)$] cm^{-1}. ^{1}H NMR ([D$_6$]-DMSO): δ = 7.40 (s, 1 H, 3-H), 7.80 (d, 2 H, 5-H and 9-H), 7.66 (d, 2 H, 6-H and 8-H) ppm. ^{13}C NMR ([D$_6$]DMSO): δ = 182.1 (C-1), 140.6 (C-2), 132.3 (C-3), 137.2 (C-4), 132.5 (C-5 and C-9), 136.5 (C-6 and C-8), 91.5 (C-7) ppm.

[Pb(CH$_3$O-pspa)]: Yellow solid, yield 95%. $C_{10}H_8O_3PbS$ (415.45): calcd. C 28.91, H 1.94, S 7.72; found C 28.80, H 1.90, S 7.49. MS (FAB): *m/z* (%) = 417 (49) [Pb(CH$_3$O-pspa) + H]$^+$. IR (KBr): $\tilde{\nu}$ = 1503 [vs, $\nu_a(CO_2^-)$], 1329 [s, $\nu_s(CO_2^-)$] cm^{-1}. ^{1}H NMR ([D$_6$]DMSO): δ = 7.45 (s, 1 H, 3-H), 7.94 (d, 2 H, 5-H and 9-H), 6.90 (d, 2 H, 6-H and 8-H), 3.75 (s, 3 H, CH$_3$O) ppm. ^{13}C NMR ([D$_6$]DMSO): δ = 182.9 (C-1), 135.1 (C-2), 133.9 (C-3), 130.3 (C-4), 131.9 (C-5 and C-9), 113.9 (C-6 and C-8), 157.6 (C-7), 54.9 CH$_3$O ppm.

[Pb(F$_3$CO-pspa)]: Yellow solid, yield 82%. $C_{10}H_5F_3O_3PbS$ (469.42): calcd. C 25.59, H 1.07, S 6.83; found C 25.94, H 0.91, S 6.40. MS (FAB): *m/z* (%) = 471 (50) [Pb(F$_3$CO-pspa) + H]$^+$. IR (KBr): $\tilde{\nu}$ = 1506 [vs, $\nu_a(CO_2^-)$], 1314 [vs, $\nu_s(CO_2^-)$] cm^{-1}. ^{1}H NMR ([D$_6$]-DMSO): δ = 7.50 (s, 1 H, 3-H), 8.90 (d, 2 H, 5-H and 9-H), 7.31 (d, 2 H, 6-H and 8-H) ppm. ^{13}C NMR ([D$_6$]DMSO): δ = 182.1 (C-

© 2013 Wiley-VCH Verlag GmbH & Co. KGaA, Weinheim

1), 140.5 (C-2), 131.9 (C-3), 137.2 (C-4), 132.1 (C-5 and C-9), 120.4 (C-6 and C-8), 146.1 (C-7), 120.2 (q, $^1J_{^{13}C,^{19}F}$ = 255.8 Hz, OCF_3) ppm.

[Pb(HO-pspa)]: Red solid, yield 74%. $C_9H_6O_3PbS$ (401.43): calcd. C 26.93, H 1.51, S 7.99; found C 26.72, H 1.73, S 7.95. MS (FAB): *m/z* (%) = 402 (4) $[Pb(OH\text{-}pspa) + H]^+$. IR (KBr): $\tilde{\nu}$ = 1493 [vs, $\nu_a(CO_2^-)$], 1329 [vs, $\nu_s(CO_2^-)$] cm^{-1}. ^1H NMR ([D$_6$]DMSO): δ = 7.43 (s, 1 H, 3-H), 7.82 (d, 2 H, 5-H and 9-H), 6.72 (d, 2 H, 6-H and 8-H), 9.48 (br s, 1 H, 7-OH) ppm. ^{13}C NMR ([D$_6$]DMSO): δ = 183.2 (C-1), 133.6 (C-2), 134.6 (C-3), 128.7 (C-4), 132.2 (C-5 and C-9), 114.7 (C-6 and C-8), 156.1 (C-7) ppm.

The $[HQ]_2[Pb(X\text{-}pspa)_2]$ complexes were prepared by following the same general method: to a mixture of lead(II) acetate trihydrate and diisopropylamine (Q) in ethanol was added a solution of the appropriate sulfanylcarboxylic acid in the same solvent until a molar ratio of ca. 1:4:2 was achieved. The mixture was stirred at room temperature, and the resulting solid was separated by centrifugation and dried under vacuum. For example, to a mixture of lead(II) acetate trihydrate (0.18 g, 0.47 mmol) and diisopropylamine (Q, 0.26 mL, 1.9 mmol) in ethanol (15 mL) was added a solution of H_2(Cl-pspa) (0.20 g, 0.93 mmol) in ethanol (15 mL). The mixture was stirred for 3 h, and the resulting solid was isolated.

$[HQ]_2[Pb(Cl\text{-}pspa)_2]$: Beige solid, yield 48%. $C_{30}H_{42}Cl_2N_2O_4S_2Pb$ (836.93): calcd. C 43.06, H 5.06, N 3.35, S 7.66; found C 43.55, H 5.57, N 3.42, S 8.03. MS (FAB): *m/z* (%) = 421 (10) $[Pb(Cl\text{-}pspa) + H]^+$. MS (ESI+): *m/z* = 710 (2) $[Pb(Cl\text{-}pspa)_2 + DMSO + 3H]^+$, 635 (5) $[Pb(Cl\text{-}pspa)_2 + 3H]^+$, 498 (2) $[Pb(Cl\text{-}pspa) + DMSO + H]^+$, 443 (4) $[Pb(Cl\text{-}pspa) + Na]^+$, 421 (100) $[Pb(Cl\text{-}pspa) + H]^+$. MS (ESI–): *m/z* (%) = 871 (4) $[Pb(Cl\text{-}pspa)_3 + 2H + Na]^-$, 847 (26) $[Pb(Cl\text{-}pspa)_3 + 3H]^-$, 633 (37) $[Pb(Cl\text{-}pspa)_2 + H]^-$, 480 (100) [(Cl-pspa–$S_3$–pspa-Cl) + Na]$^-$, 449 (5) [(Cl-pspa-S–S-pspa-Cl) + Na]$^-$, 427 (86) [(Cl-pspa-S–S-pspa-Cl) + H]$^-$, 383 (8) [(Cl-pspa-S–S-pspa-Cl)–COO + H]$^-$, 319(3) [(Cl-pspa-S–S-pspa-Cl)–COOH–COSH + H]$^-$. IR (KBr): $\tilde{\nu}$ = 1609 [vs, $\delta(NH_2^+)$], 1520 [vs, $\nu_a(CO_2^-)$], 1317 [vs, $\nu_s(CO_2^-)$] cm^{-1}. ^1H NMR ([D$_6$]DMSO): δ = 7.38 (s, 2 H, 3-H), 8.06 (d, 4 H, 5-H and 9-H), 7.29 (d, 4 H, 6-H and 8-H), 1.18 (d, 24 H, CH_3), 3.29 (sept, 4 H, CH), 8.92 (br s, 4 H, NH_2^+) ppm. ^{13}C NMR ([D$_6$]DMSO): δ = 179.9 (C-1), 143.8 (C-2), 129.1 (C-3), 137.7 (C-4), 131.2 (C-5 and C-9), 127.3 (C-6 and C-8), 131.2 (C-7), 19.1 (CH_3 HQ), 45.8 (CH HQ) ppm. Single crystals were grown by slow evaporation of the mother liquor.

$[HQ]_2[Pb(Br\text{-}pspa)_2]$: Beige solid, yield 54%. $PbC_{30}H_{42}Br_2N_2O_4S_2$ (925.83): calcd. C 38.92, H 4.57, N 3.03, S 7.22; found C 38.76, H 4.67, N 3.02, S 6.93. MS (FAB): *m/z* (%) = 465 (54) $[Pb(Br\text{-}pspa) + H]^+$. MS (ESI+): *m/z* (%) = 803 (6) $[Pb(Br\text{-}pspa)_2 + DMSO + 3H]^+$, 725 (6) $[Pb(Br\text{-}pspa)_2 + 3H]^+$, 541 (8) $[Pb(Br\text{-}pspa) + DMSO + H]^+$, 487 (4) $[Pb(Br\text{-}pspa) + Na]^+$, 465 (100) $[Pb(Br\text{-}pspa) + H]^+$. MS (ESI–): *m/z* (%) = 1004 (2) $[Pb(Br\text{-}pspa)_3 + 2H + Na]^-$, 745 (16) $[Pb(Br\text{-}pspa)_2 + Na]^-$, 723 (21) $[Pb(Br\text{-}pspa)_2 + H]^-$, 570 (100) [(Br-pspa–$S_3$–pspa-Br) + Na]$^-$, 537 (8) [(Br-pspa-S–S-pspa-Br) + Na]$^-$, 515 (57) [(Br-pspa-S–S-pspa-Br) + H]$^-$, 471 (7) [(Br-pspa-S–S-pspa-Br)–COO + H]$^-$, 425 (5) [(Br-pspa-S–S-pspa-Br)–COOH–COSH + H]$^-$, 258 (5) [HBr-pspa]$^-$, 257 (4) [(Br-pspa-S–S-pspa-Br)]$^{2-}$. IR (KBr): $\tilde{\nu}$ = 1609 [vs, $\delta(NH_2^+)$], 1522 [vs, $\nu_a(CO_2^-)$], 1315 [vs, $\nu_s(CO_2^-)$] cm^{-1}. ^1H NMR ([D$_6$]DMSO): δ = 7.43 (s, 2 H, 3-H), 8.02 (d, 4 H, 5-H and 9-H), 7.40 (d, 4 H, 6-H and 8-H), 1.20 (d, 24 H, CH_3), 3.32 (sept, 4 H, CH), 8.23 (br s, 4 H, NH_2^+) ppm. ^{13}C NMR ([D$_6$]DMSO): δ = 179.3 (C-1), 144.3 (C-2), 129.3 (C-3), 137.8 (C-4), 131.5 (C-5 and C-9), 130.3 (C-6 and C-8), 117.5 (C-7), 19.2 (CH_3 HQ), 46.0 (CH HQ) ppm. Single crystals were grown by slow evaporation of the mother liquor.

X-ray Crystal Structure Determination Studies: Single crystals were mounted on glass fibres in a Bruker APEXII automatic diffractometer, and data were collected at 293 K (or 110 K) with Mo-K_α radiation (λ = 0.71073 Å). Corrections for Lorentz effects, polarization[42] and absorption[43] were made.

Structure analyses were performed by direct methods.[44] Least-squares full-matrix refinements on F^2 were performed by using the program SHELXL97.[44] Atomic scattering factors and anomalous dispersion corrections for all atoms were taken from *International Tables for Crystallography*.[45] All non-hydrogen atoms were refined anisotropically. Hydrogen atoms were refined as riders at geometrically calculated positions. Graphics were obtained with ORTEP-3[46] and MERCURY.[47] The main crystal and refinement parameters for the compounds are given in Tables 3 and S3.

Table 3. Crystal and refinement data for $[H_2(Cl\text{-}pspa)]$ and $[HQ]_2[Pb(Cl\text{-}pspa)_2]$.

Compound	$[H_2(Cl\text{-}pspa)]$	$[HQ]_2$ $[Pb(Cl\text{-}pspa_2)]$
Empirical formula	$C_9H_7ClO_2S$	$C_{30}H_{42}Cl_2N_2O_4PbS_2$
M	214.66	836.87
T [K]	293(2)	110.0(1)
Crystal system	triclinic	monoclinic
Space group	$P\bar{1}$	$P2_1/c$
a [Å]	5.8339(14)	21.363(5)
b [Å]	9.069(2)	10.531(3)
c [Å]	9.940(3)	15.110(4)
α [°]	111.421(4)	
β [°]	104.628(4)	97.227(4)
γ [°]	93.247(4)	
V [Å^3]	467.2(2)	3372.3(15)
Z	2	4
$D_{calcd.}$ [Mg/m^3]	1.526	1.648
μ [mm^{-1}]	0.592	5.321
F (000)	220	1664
Crystal size [mm]	0.40 × 0.30 × 0.23	0.12 × 0.10 × 0.05
θ range for data collection [°]	2.30 to 28.02	1.92 to 26.37
Reflections collected	3047	37283
Unique reflections, $[R_{(int)}]$	2131 [0.0179]	6866 [0.0823]
Final R_1, wR_2 $[I > 2\sigma(I)]$	0.0467, 0.1206	0.0367, 0.0776

CCDC-922806 [for H_2(Cl-pspa)], -922807 {for $[HQ]_2[Pb(Cl\text{-}pspa)_2]$} and -922808 {for $[HQ]_2[Pb(Br\text{-}pspa)_2]$} contain the supplementary crystallographic data for this paper. These data can be obtained free of charge from The Cambridge Crystallographic Data Centre via www.ccdc.cam.ac.uk/data_request/cif.

Supporting Information (see footnote on the first page of this article): Crystallographic data for $[HQ]_2[Pb(Br\text{-}pspa)_2]$.

Acknowledgments

The authors would like to thank the Spanish Ministry of Education and Science (MEC) for financial support under Project CTQ 2006-11805, the Spanish Ministry of Education and Innovation (MICINN) for Project CTQ 2009-10738, and the Dirección Xeral de I+D, Xunta de Galicia, Spain (IN845B-2010/121).

[1] R. P. Wedeen, *Int. J. Occup. Environ. Med.* **2011**, *2*, 1–3.
[2] D. C. Bellinger, *Int. J. Environ. Res. Public Health* **2011**, *8*, 2593–2628.

 © 2013 Wiley-VCH Verlag GmbH & Co. KGaA, Weinheim

[3] M. S. Sinicropi, D. Amantea, A. Caruso, C. Soturnino, *Arch. Toxicol.* **2010**, *84*, 501–520.
[4] S. Bradberry, T. Sheehan, A. Vale, *QJM* **2009**, *102*, 721–732.
[5] O. Andersen, *Chem. Rev.* **1999**, *99*, 2683–2710.
[6] S. J. S. Flora, G. Flora, G. Saxena, in: *Lead, Chemical, Analytical Aspects, Environmental Impact and Health Effects* (Eds.: J. S. Casas, J. Sordo), Elsevier, Amsterdam, **2006**, p. 158–228.
[7] R. L. Davidovich, *Russ. J. Coord. Chem.* **2005**, *31*, 455–466.
[8] A. C. Schell, M. Parvez, F. Jalilehvand, *Acta Crystallogr., Sect. E* **2012**, *68*, m489–m490.
[9] X. Fang, Q. Fernando, *Chem. Res. Toxicol.* **1995**, *8*, 525–536.
[10] J. S. Casas, J. Sordo, M. J. Vidarte, in: *Lead, Chemical, Analytical Aspects, Environmental Impact and Health Effects* (Eds.: J. S. Casas, J. Sordo), Elsevier, Amsterdam, **2006**, p. 41–99.
[11] J. A. Lewis, S. Cohen, *Inorg. Chem.* **2004**, *43*, 6534–6536, and references cited therein.
[12] R. Tofighi, C. Johansson, M. Goldoni, W. N. W. Ibrahim, V. Gogvadze, A. Mutti, S. Ceccatelli, *Neurotox. Res.* **2011**, *19*, 183–194.
[13] J. S. Casas, M. V. Castaño, M. D. Couce, A. Sánchez, J. Sordo, M. D. Torres, E. M. Vázquez López, *Eur. J. Inorg. Chem.* **2012**, 4822–4832.
[14] M. F. Camiña, J. S. Casas, M. V. Castaño, M. D. Couce, A. Gato, P. Herbello-Hermolo, A. Sánchez, J. Sordo, M. D. Torres, *J. Inorg. Biochem.* **2010**, *104*, 599–610.
[15] A. Izquierdo, L. García Puignou, *An. Quim.* **1983**, *72B*, 254–259.
[16] B. Cordero, V. Gómez, A. E. Platero-Prats, M. Revés, J. Echeverría, E. Cremades, F. Barragán, S. Alvarez, *Dalton Trans.* **2008**, 2832–2838.
[17] J. S. Casas, E. E. Castellano, M. D. Couce, M. García-Vega, A. Sánchez, A. Sánchez-Gonzalez, J. Sordo, J. M. Varela, E. M. Vázquez-López, *Dalton Trans.* **2010**, *39*, 3931–3943.
[18] E. Barreiro, J. S. Casas, M. D. Couce, A. Sánchez, R. Seoane, J. Sordo, J. M. Varela, E. M. Vázquez-López, *Eur. J. Med. Chem.* **2008**, *43*, 2489–2497.
[19] T. Steiner, *Acta Crystallogr., Sect. C* **2000**, *56*, 876–877.
[20] B. M. Kariuki, C. L. Bauer, K. D. M. Harris, S. J. Teat, *Angew. Chem.* **2000**, *112*, 4659; *Angew. Chem. Int. Ed.* **2000**, *39*, 4485–4488.
[21] A. Bondi, *J. Phys. Chem.* **1964**, *68*, 441–451.
[22] L. Shimoni-Livny, J. P. Glusker, C. W. Block, *Inorg. Chem.* **1998**, *37*, 1853–1857.
[23] a) S. Rupprecht, K. Langemann, T. Lügger, J. M. McCormick, K. N. Raymond, *Inorg. Chim. Acta* **1996**, *243*, 79–90; b) K. Abu-Dari, T. B. Karpishin, N. K. Raymond, *Inorg. Chem.* **1993**, *32*, 3052–3055; c) K. Abu-Dari, F. E. Hahn, K. N. Raymond, *J. Am. Chem. Soc.* **1990**, *112*, 1519–1524.
[24] a) X.-Y. Yu, H.-H. Zou, L.-Q. Wei, M.-H. Zeng, *Inorg. Chem. Commun.* **2010**, *13*, 1137–1139; b) L. Zeng, Y.-Q. Chen, G.-Ch. Liu, J.-X. Zhang, *J. Mol. Struct.* **2009**, *930*, 176–179.
[25] J. S. Casas, E. E. Castellano, J. Ellena, M. S. García-Tasende, A. Sánchez, J. Sordo, A. Touceda, *Z. Anorg. Allg. Chem.* **2005**, *631*, 2247–2252.
[26] I. Y. Torshin, I. T. Weber, R. W. Harrison, *Protein Eng.* **2002**, *15*, 359–363.
[27] F. Marandi, M. Mottaghi, G. Meyer, I. Pantenburg, *Z. Anorg. Allg. Chem.* **2009**, *635*, 165–170.
[28] C. Janiak, *J. Chem. Soc., Dalton Trans.* **2000**, 3885–3896.
[29] A. I. Kitaigorodskii, *Molecular Crystals and Molecules*, Academic Press, New York, **1973**.
[30] A. L. Spek, *PLATON, A Multipourpose Crystallographic Tool*, Utrecht University, **2001**.
[31] J. S. Casas, M. V. Castaño, A. Sánchez, J. Sordo, M. D. Torres, M. D. Couce, A. Gato, C. Alvarez-Lorenzo, M. F. Camiña, E. E. Castellano, *Inorg. Chem.* **2010**, *49*, 2173–2181.
[32] J. S. Casas, A. Castiñeiras, M. D. Couce, M. L. Jorge, U. Russo, A. Sánchez, R. Seoane, J. Sordo, J. M. Varela, *Appl. Organomet. Chem.* **2000**, *14*, 421–431.
[33] K. Nakamoto, *Infrared and Raman Spectra of Inorganic and Coordinaiton Compounds*, 5th ed. part B, John Wiley & Sons, New York, **1997**, p. 60.
[34] J. S. Casas, A. Castiñeiras, M. D. Couce, N. Playá, U. Russo, A. Sánchez, J. Sordo, J. M. Varela, *J. Chem. Soc., Dalton Trans.* **1998**, 1513–1521.
[35] E. Barreiro, J. S. Casas, M. D. Couce, A. Sánchez, J. Sordo, J. M. Varela, E. M. Vázquez-López, *Dalton Trans.* **2005**, 1707–1715.
[36] V. B. di Marco, G. G. Bombi, *Mass Spectrom. Rev.* **2006**, *25*, 347–379.
[37] C. Liu, Y. Ouyang, B. Jia, Z. Zhu, J. Shi, H. Chen, *J. Mass Spectrom.* **2012**, *47*, 769–777.
[38] E. Barreiro, J. S. Casas, M. D. Couce, A. Sánchez, J. Sordo, J. M. Varela, E. M. Vázquez-López, *Cryst. Growth Des.* **2007**, *7*, 1964–1973.
[39] J. S. Casas, A. Castiñeiras, M. D. Couce, M. García-Vega, M. Rosende, A. Sánchez, J. Sordo, J. M. Varela, E. M. Vázquez-López, *Polyhedron* **2008**, *27*, 2436–2446.
[40] a) B. L. Sharma, D. N. Kachru, S. Sing, S. K. Tandon, *J. Appl. Toxicol.* **1986**, *6*, 253–257; b) B. L. Sharma, S. Khandelwal, D. N. Kachru, S. Singh, S. K. Tandon, *Jpn. J. Pharmacol.* **1987**, *45*, 295–302; c) D. N. Kachru, S. Singh, S. K. Tandon, *Toxicol. Lett.* **1991**, *57*, 251–256.
[41] H.-H. Lee, A. Kuwae, K. Hanai, *Spectrosc. Lett.* **1994**, *27*, 787–799.
[42] *SAINT, SAX Area Detector Integration*, Bruker Analytical Instrumentation, **1996**.
[43] A. C. T. North, D. C. Phillips, F. S. Mathews, *Acta Crystallogr., Sect. A* **1968**, *24*, 351–359.
[44] *SHELXS97* and *SHELXL97*, *Programs for the Refinement of Crystal Structures*: G. M. Sheldrick, University of Göttingen, Germany, **1997**.
[45] *International Tables for X-ray Crystallography*, vol. C, Kluwer Academic Publishers, Dordrecht, The Netherlands, **1995**.
[46] *ORTEP III* for Microsoft Windows®: J. L. Farrugia, *J. Appl. Crystallogr.* **1997**, *30*, 565.
[47] *Mercury*, v. 1.4.2, *A Program for crystal structure visualization and exploration*, The Cambridge Crystallographic Data Centre, Cambridge, UK.

Received: May 16, 2013
Published Online: August 16, 2013

 © 2013 Wiley-VCH Verlag GmbH & Co. KGaA, Weinheim